PERGAMON

International Journal of Heat and Mass Transfer 43 (2000) 2205–2220

International Journal of HEAT and MASS TRANSFER

www.elsevier.com/locate/ijhmt

An experimental identification of line heat sources in a diffusive system using the boundary element method

C. Le Niliot [a,*], F. Rigollet [a], D. Petit [b]

[a] *Institut Universitaire des Systèmes Thermiques Industriels, UMR CNRS 6595 Technopôle de Château Gombert, 5 Rue Enrico Fermi, 13 453 Marseille Cedex 13, France*

[b] *Laboratoire d'Etudes Thermiques, UMR CNRS 6608, BP 109, 86 960 FUTUROSCOPE Cedex, France*

Received 25 November 1998; received in revised form 29 July 1999

Abstract

This paper deals with an inverse problem which consists of the experimental identification of line heat source strength in an homogeneous solid using temperature measurements. An inverse formulation using the boundary element method, is used to identify the strength of line heat sources. In the case of multiple sources identification the location is assumed to be known but, in the case of a single source, an iterative algorithm for the location identification is proposed. The experiment consists of the identification of the power dissipated by Joule effect in one or two thin wires placed in a long square section cement bar. The measurements necessary to solve the inverse problem are provided by thermocouples for the internal temperatures and by infrared thermography for the superficial temperatures. A time regularization procedure associated to future time steps is used to correctly solve the ill-posed problem.

1. Introduction

Given the partial differential equation governing the heat transfer phenomena, the direct problem consists of the determination of the temperature field in a domain Ω knowing: the geometry, the initial condition, all the boundary conditions, the heat generation term and the thermophysical parameters (diffusivity and conductivity for example).

When one of these functions or parameters is unknown the problem is called inverse. In the inverse problem the aim is the reconstruction of an unknown function or an unknown parameter knowing some temperature or flux measurements [1,2].

Our contribution to Inverse Heat Conduction Problem (IHCP) resolution consists of a formulation using the Boundary Element Method (BEM). In [3,4] BEM is applied to unknown boundary conditions reconstruction and in [5] to point heat source strength identification. In [5] only simulated results are presented, in the present work we propose an experimental application of BEM applied to point heat source strength identification.

In the case of a single source we present an iterative procedure to identify the line heat source position. This method, valid for the single source identification, has been presented in [6,7] using a

Abbreviations: BEM, Boundary Element Method; BIE, Boundary Integral Equation; IHCP, Inverse Heat Conduction Problem; niter, number of iterations.

* Corresponding author.

E-mail address: c12@iusti-univ-mrs.fr (C. Le Niliot).

0017-9310/00/$ - see front matter
PII: S0017-9310(99)00285-9

Nomenclature

A linear system matrix
B second member vector
c multiplying coefficient
C diagonal matrix
d distance from the line heat source (m)
g heat source term (W m^{-3})
g line heat source strength (W m^{-1})
h heat transfer coefficient (W m^{-2} K^{-1})
H **G**; matrices of transient BIE
I matrix for point source treatment
K number of point sources
N boundary elements number
N' internal points number
p heat flux density (W m^{-2})
P heat flux densities vector
q^* normal derivative of T^*
Q time regularization matrix
R number of future time steps
S source terms vector
t time (s)
T temperature vector
T^* fundamental solution
U space regularization matrix
W second member vector
X solution vector

Greek symbols
α thermal diffusivity (m^2 s^{-1})
δ Dirac function
ϵ emissivity
Γ boundary of the diffusive domain
λ conductivity (W m^{-1} K^{-1})
η time regularization coefficient
μ space regularization coefficient
θ temperature (°C)
σ standard deviation
Ω diffusive domain

Subscripts
0 initial time
k point source index
f time index
F final time
r future time step index
∞ ambient conditions

Superscript
$'$ internal points

deconvolution procedure. Here, the method is applied to our experiment for the single source case, while for the two sources case, the location of the sources are assumed to be known. We present in this paper an academic 2-D application, a down to earth application could be the identification of cracks in a system submitted to vibrations. The stressed system produces, at the crack location, a heat generation which could be detected by our approach.

Due to the ill-posed nature of the inverse problem, the timewise variation estimation of the point heat source intensity is highly sensitive to measurement errors. In order to correctly identify the source strength, we use the regularization procedure recommended by Thikonov [8]. This procedure is applied to the solution over some future time steps.

The experiment consists of a long bar of cement crossed by a thin heating wire. The aim of the inverse problem is to identify the position of the wire and the time variation of the power dissipated by Joule effect. The line heat source represented by the heating wire can be approximated by a point in the 2-D central section. To solve the inverse problem, some temperature measurements are necessary: internal measurements provided by thermocouples and superficial measurements provided by an infrared scanner.

In order to correctly solve the inverse problem using only temperature measurements, it is necessary to know the thermophysical properties of the material as accurately as possible. This is the reason why a parameter estimation procedure is applied to the experimental set-up.

In the first part of the work we present in detail the experimental design under investigation. The second part describes the location identification algorithm and the associated experimental results. The third part surveys BEM formulation for point heat source strength identification which is detailed in [5]. In this last part the presentation of the inverse method is followed by the results obtained with our 2-D experimental test case.

2. A 2-D experiment using infrared thermographic data and internal temperatures

In order to test the identification method proposed in [5], an experiment has been set up. This experiment also enables the position identification algorithm to be validated. The experimental design is a long bar

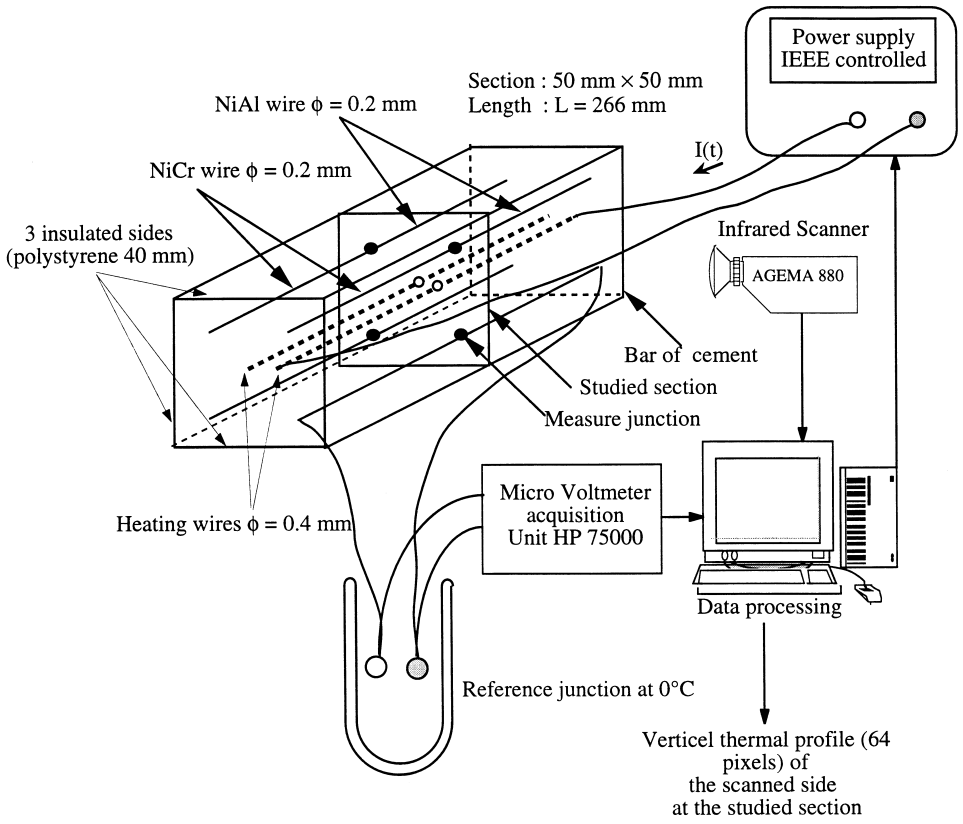

Fig. 1. The experimental design.

crossed at its longest dimension by a thin heating wire. The chosen material is cement which leads to measurable temperature gradients in the material with reasonable fluxes.

The BEM approach for solving inverse problems has to be implemented with the thermophysical parameters λ and α. The problem is that with this type of material the thermophysical parameters depend on many factors: porosity, moisture percentage, sand percentage ... Then, conductivity and diffusivity have to be identified 'in situ' using a parameter estimation procedure.

2.1. The experimental design

The experimental design under investigation is a long square section bar of cement crossed at its longest dimension by two KANTHAL® heating wires 0.4 mm in diameter. In the central section of the bar, the diffusion system is bidimensional. Considering the heating wire diameter (0.4 mm) compared to the section of the bar (50 mm × 50 mm), the heat generation can be approximated by a point in a section (see Fig. 1). Three sides of the bar are insulated by a solid foam (polystyrene) 40 mm thick. The fourth side is scanned by an infrared AGEMA 880 scanner.

In the section under investigation five interior sensors can be found at the positions displayed in Fig. 2.

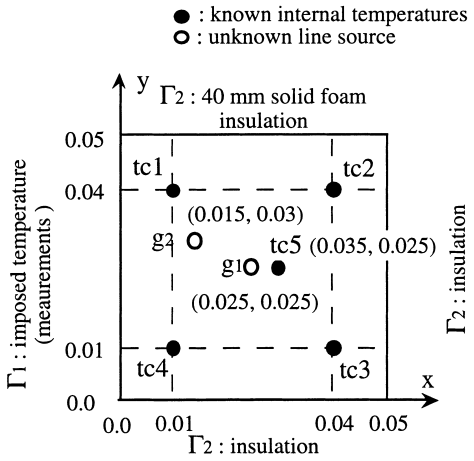

Fig. 2. Sensors location and boundary conditions in the studied section.

The five sensors are K type thermocouples of 0.2 mm diameter. The fifth sensor tc5 is not used to identify the heat sources strength but the thermophysical parameters. This one is placed at about 1 cm of source g1 in order to have a good signal level at short times. The sensors locations are chosen to have a complete information in the body without any knowledge of the point heat source location. To reduce the perturbation of the thermocouples on the temperature field, they are placed along an isothermal line.

The electrical insulation is made by a plastic varnish, and the measurement junction is located at the centre of the bar as shown in Fig. 1. Two types of temperature data can be used: surface temperatures corresponding to the scanned surface, and the four internal measurements corresponding to four internal points.

The surface temperature is measured using an infrared scanner AGEMA 880, the scanned surface is painted with a black paint of emissivity $\epsilon = 0.98$. Infrared pictures are made of 64×128 pixels (picture elements), in this datafile it is necessary to extract 10 values representing the 10 boundary elements over the surface of the bar. To obtain this information from the picture we use a quadratic interpolation over the vertical profile at the studied section. The average temperature is then calculated at the middle of the element in respect of the constant element approximation used by the BEM formulation. Only the vertical thermal profile at the studied section is used, what is left of the infrared picture is ignored. The maximum picture acquisition frequency is 6.25 Hz which represents a period of 0.16 s. In our application, the chosen acquisition period is 25.28 s representing one picture every 158. To get a constant time step of 40 s, a linear approximation on time is used.

Internal measurements are obtained using a digital micro voltmeter associated to a relay card. The reference junction is kept at 0°C in a dewar bowl containing melting ice. Temperature is calculated using a 6th order approximation of the reference table for K type thermocouple between 0 and 200°C. Results are transferred to a micro computer using an IEEE link.

The energy is provided by a double HP-IB® controlled power supply. Current intensity (from 0 to 3.5 A) is imposed by the generator and the voltage is measured by the acquisition unit. Current in the wires is imposed in the same acquisition program as temperatures which gives a good synchronism between solicitation and measurements. For sinusoidal or triangular solicitations, intensity is calculated and changed every 0.2 s (approximately) which leads to a good approximation of the chosen function shape. In all the following, the acquisition time is measured with a period of about 10 s. A linear interpolation is used to get a period equal to the BEM program, here 40 s.

As the system can be considered 2-D at the centre of the bar, the heat source value is: $\mathbf{g} = Vi/L$, with $\mathbf{g}$ the power in W/m, V the measured tension in V, i the current intensity in A and L the length of the bar (0.266 m).

2.2. The experimental inverse problem

Two examples are presented in this paper: the first one concerns a single source (g_1 or g_2) identification (location and strength), the second one is related to the simultaneous identification of g_1 and g_2 intensities. In all these cases we will use the same mesh and the same boundary conditions. In this paragraph we present the boundary conditions used to solve the inverse problem. To modelize the experiment under investigation the computational domain is discretized in 40 BEM linear elements (10 per side of the square).

The inverse problem consists of solving the fundamental heat transfer equation using the following boundary conditions:

- at $t = 0$: known homogeneous initial temperature $\theta(x, y, 0) = \theta_\infty$ and at the boundary;
- on Γ_2: imperfect insulation (40 mm polystyrene) with $-\lambda(\partial\theta/\partial n) = h(\theta_\infty - \theta)$;
- on Γ_1, known temperatures (measurements from infrared thermography);
- four internal temperatures $\theta'(x_i, y_i, t)$ measured at locations tc1, tc2, tc3, tc4;
- inside the domain, one or two line heat sources of *unknown* strength $\mathbf{g}_k(t)$.

For the cases involving a single source the position can be identified using an iterative method, for the double source case the positions are assumed to be known. It can be noticed that the introduced set of boundary conditions does not involve any assumption concerning the heat flux at boundary Γ_1. Nevertheless some heat losses are taken into account on the boundary. Heat loss coefficient h is identified using a numerical procedure as described in [6,7]. This numerical procedure consists of a minimization based on steady state measurements in order to take into account the heat losses through the insulation. The insulation is made by 40 mm of polystyrene foam. Some steady state measurements associated to a minimization procedure using the above mentioned boundary conditions leads to the heat losses coefficient: $h = 2.6\ \mathrm{W\ m^{-2}\ K^{-1}}$. A direct modelization of the 2-D heat transfers through the foam would give similar results for the average overall heat losses coefficient. In this case as the steady state is never reached a global constant heat transfer of $2.6\ \mathrm{W\ m^{-2}\ K^{-1}}$ is sufficient to modelize the diffusive losses through the solid foam insulation.

As the studied diffusive system is made of cement, it is necessary to accurately identify the thermal par-

ameters: the diffusivity and the conductivity. This is the purpose of the following paragraph.

2.3. The thermophysical parameter identification

In order to have the most accurate values of thermal conductivity λ and thermal diffusivity α of the cement bar, these are identified with the same experimental set up. Wire $g1$ located at the centre of the bar is heated for a finite duration and the temperature rise is measured by tc5 inside the solid at a distance d from the heating wire. The experimental temperature history is compared to the theoretical one calculated by a direct model depending on the two parameters. A non-linear parameter estimation method enables then to identify the unknown conductivity and diffusivity.

Since we are interested in the central section of the bar, the wire can be considered as an infinite line heat source. Moreover, for short enough times, the bar can be considered as an infinite radius cylinder and heat transfer can be described by a 1D radial model, in cylindrical coordinates with origin on the heating wire [9]. The temperature rise θ at distance d from the heating wire that delivers the constant heat flux $\mathbf{g}$ for a finite duration is then analytically calculated using the superposition theorem.

In order to ensure the minimal area of the confidence region of the estimates, the experimental parameters to optimize are the duration of heating and the maximum time at which data are used. This optimization procedure is performed as recommended in [10,11].

In our experiment, the wire is heated during 101.56 s and data are finally used until 179.5 s. The corresponding values of estimates λ and α are presented in Table 1. For this experiment the residuals distribution can be well approached by a zero mean normal distribution. That enables assumptions to be validated on measurement errors distribution and to estimate its standard deviation $\sigma = 0.0085$ K that indicates measurements of good quality. Taking into account the measurement errors and the errors on known parameters ($\mathbf{g} = 65.5 \pm 0.6$ W m^{-1} and $d = 9.5 \pm 0.6$ mm) leads to the results presented in Table 1.

Table 1
Identified parameters and 99% confidence intervals

$\lambda \pm \Delta\lambda$ (W m^{-1} K^{-1})	$\alpha \pm \Delta\alpha$ (m^2 s^{-1})
0.825 ± 0.007	$5.2 \times 10^{-7} \pm 0.7 \times 10^{-7}$

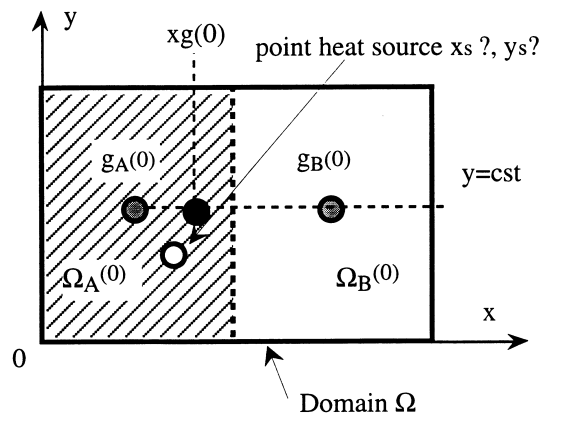

Fig. 3. Example of an iteration involving $xg(1)$ identification.

3. The point heat source location algorithm

As the thermophysical properties of the experiment are well estimated, we propose here to deal with a system containing a single point source. The aim here is to identify its position from the measurement at thermocouples tc1 to tc4 and the superficial temperatures and fluxes over the scanned surface (Γ_1 see Fig. 2). It has to be noticed that we do not use any prior information on the time variations of the source strength.

3.1. The algorithm

The method is based on the resolution of an IHCP using the measured temperatures tc1 to tc4. The aim is to solve an inverse problem using these temperatures in order to identify the strength of two separated artificial heat sources g_A and g_B located in the diffusive domain Ω (see Figs. 3 and 4). That corresponds to a

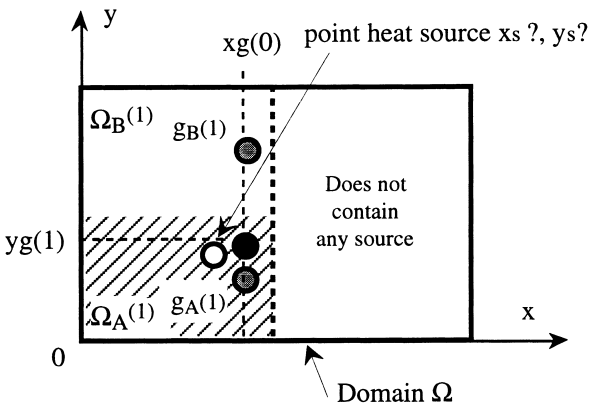

Fig. 4. Example of an iteration involving $yg(1)$ identification.

partition Ω_A, Ω_B of domain Ω. As the measured temperatures come from a single source, the identification of the strengths will point out one source rather than the other one, the pointed source is supposed to be the nearest of the real source. For the example described at Fig. 3 the part of the domain supposed to contain the searched heat source is Ω_A, two other artificial sources are set in Ω_A and the procedure can be resumed. To achieve the iterative process we assume that there is only one heat source in the domain Ω and that the heat source strength is positive.

It is important to notice that the IHCP is solved in the sense of a double heat source strength identification. The domain, the boundary mesh and the boundary conditions are the same during the iterative process, the only variables are the double heat source locations. The inverse method used here can be a linear Beck method [1,6] or BEM [5] described at section 4. The inverse method consists here in a two sources intensity identification using future time steps procedure of [1] and a regularization operator.

Using the above mentioned procedure of elimination of the supposed heat source location, the possible domain is reduced to a point, the location of this point is the identified location of the single source.

For a 2-D Cartesian geometry the algorithm can be described as follows.

1. The 2-D domain Ω is divided in two fictive parts $\Omega_A^{(0)}$ and $\Omega_B^{(0)}$ (for example parallel to Oy see Fig. 3). Each part is supposed to contain one source.
2. Two point heat sources $g_A^{(0)}$ and $g_B^{(0)}$ are created and supposed located at two points, one in each fictive part (here at y = constant).
3. The inverse problem is solved on the entire domain Ω in the sense of the strengths identification of $g_A^{(0)}$ and $g_B^{(0)}$. The identification is performed for F time steps by solving the IHCP on the domain Ω using an inverse method. As a result, the strengths of $g_A^{(0)}$ and $g_B^{(0)}$ are known for each time t_f ($0 \le t_f \le t_F$).
4. When the strengths are known, it is possible to calculate the centre of gravity of the two point sources. In a cartesian geometry for instance if y = constant we have:

$$x_g^{(1)} = \frac{\sum_{f=1}^{F}(g_A^{(0)}(f)x_A^{(0)} + g_B^{(0)}(f)x_B^{(0)})}{\sum_{f=1}^{F}(g_A^{(0)} + g_B^{(0)})}. \quad (1)$$

5. The part of domain Ω which does not contain $x_g^{(1)}$ is supposed to not contain any source and is excluded (for example here part B) of the location identification process. The other part, supposed to contain the heat source, is then divided in two parts $\Omega_A^{(1)}$ and $\Omega_B^{(1)}$ (with a parallel to Ox, see Fig. 4) and the next iteration will concern the $y_g^{(1)}$ value. In the next iterations the excluded parts still remain for the resolution of the inverse problem which is performed on the entire domain Ω without any modification of the boundary conditions.
6. The algorithm is reproduced until the process described above converges toward a single point (according to a chosen criterion). After some iterations (niter) the coordinates of this point $x_g^{(\text{niter})}$ $y_g^{(\text{niter})}$ are supposed to be the searched point heat source coordinates x_s and y_s. Let us notice that the sum

$$\sum_{f=1}^{F}(g_A^{(k)}(f) + g_B^{(k)}(f)),$$

calculated at iteration k is also a mean to follow the convergence. In fact, this sum tends towards constant when the point source is located. That gives a supplementary criterion to stop the iterative process.

7. When the location is identified we can find the intensity by solving the inverse problem for all the time steps using the deconvolution method [6] or BEM [5].

3.2. The experimental location identification

The method previously described is applied to our experiment (see Fig.2). Two different experiments have been performed separately: a step of 96 W m^{-1} on g1 and a step on g2. For each case, the aim is to find the location of the sources from the knowledge of measured temperatures from tc1 to tc4 (see Fig. 2).

For the first case g1 whose real coordinates are $x_{g1} = 25$ mm and $y_{g1} = 25$ mm, we found: R = 4, niter = 18, average strength = 94 W m^{-1}, x = 25.97 mm, y = 24.39 mm which represent in distance 1.1 mm from the supposed location of g1, this result is obtained using four future time steps and only the first time step (F = 1). The minimum error on the location is obtained for F = 7, the results are then: niter = 13, average strength = 94.4 W m^{-1}, x = 25.90 mm, y = 24.47 mm which represent in distance 1.04 mm. This result is good compared to the diameter of the heating wires (0.4 mm).

For source g2 ($x_{g2} = 15$ mm and $y_{g2} = 30$ mm), using the first time step (F = 1) and four future time steps we obtained: niter = 15, sum = 96 W m^{-1}, x = 16.23 mm, y = 29.83 mm which represent an error on the location of 1.24 mm. Using seven time steps (F = 7) we obtained for R = 4: niter = 17, x = 16.36 mm, y = 29.98 mm, average strength = 96.28 W m^{-1}. In terms of distance the error is 1.36 mm, in this case the increase of the number of time steps identified does not improve the results.

For both experiments the strength is constant. On the one hand the results obtained for g1 location are better than for g2 location, on the other hand the strength (96 W m^{-1}) is better reconstruct for g2 than for g1. The good results obtained for the location identification are due to the fact that g1 is in the centre of the square tc1 tc2 tc3 tc4. The good results obtained for g2 strength identification are due to a high sensitivity of sensor tc1 to g2 strength variations, this result will be confirmed in the following section.

For g1, the sensitivity coefficients are almost equivalent, which is not the case for g2. In Fig. 5, we present the temperature sensitivity coefficients to a position variation at the four internal sensors. The sensitivity coefficients S_x and S_y are defined as the first derivatives of temperature with respect to coordinate. With a first order approximation, we have:

$$S_x = \frac{\Delta\theta}{\Delta x} \quad \text{and} \quad S_y = \frac{\Delta\theta}{\Delta y}.$$

The curves displayed at Fig. 5 are built for a triangular variation of strengths on g1 and g2 and a variation of 1 mm on x or y. Considering g2, as we can see on Fig. 5(c) and (d), the sensitivity to the y coordinate variation is much more important than the sensitivity to the x coordinate. This is not the case for g1 for which all sensitivities are similar (see Fig. 5(a) and (b)). Nevertheless, these positions are very important for the final results and an error on g1 position has a

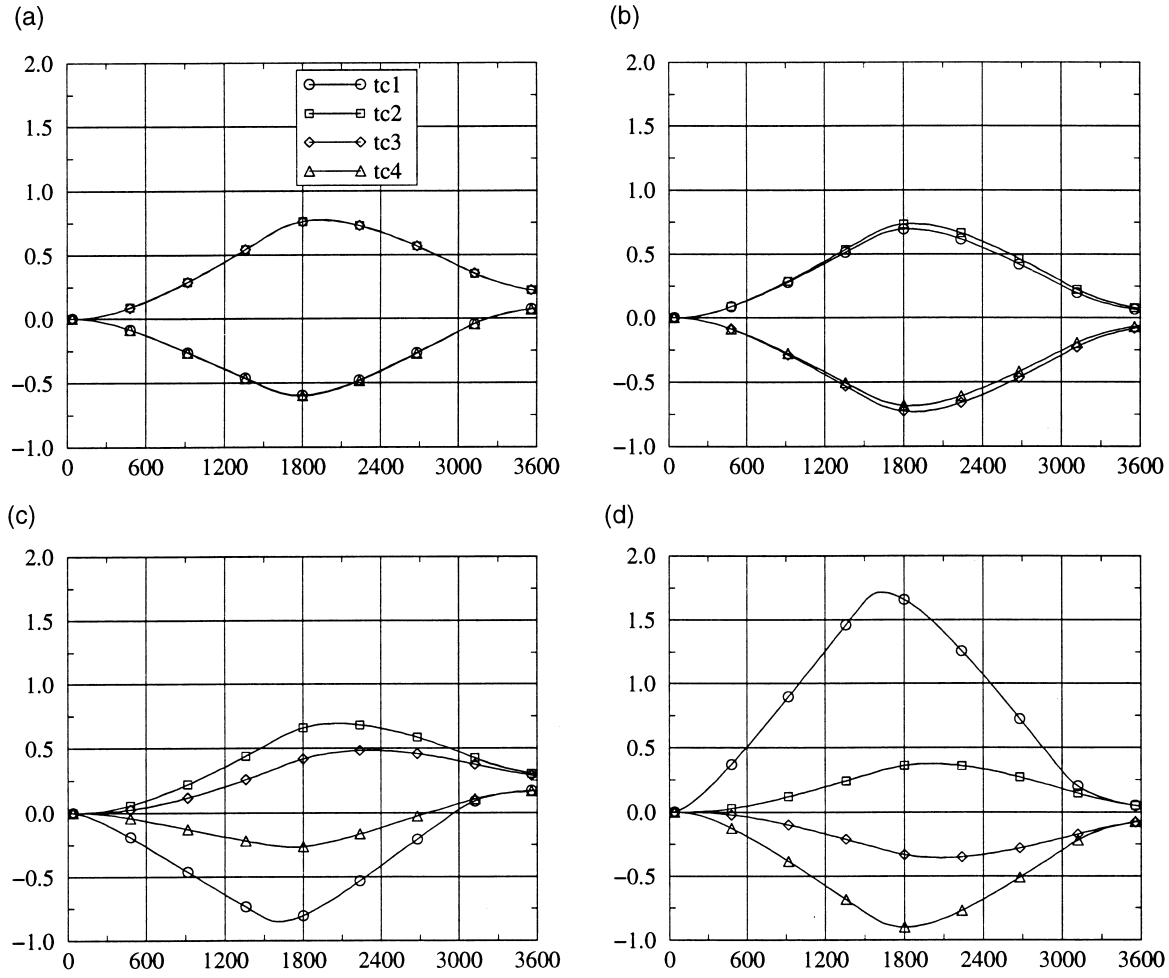

Fig. 5. Sensitivity coefficients (°C mm^{-1}) to the position vs time (s) using an exact position. (a) S_x for g1 and $\Delta x = 1$ mm; (b) S_y for g1 and $\Delta y = 1$ mm; (c) S_x for g2 and $\Delta x = 1$ mm; (d) S_y for g2 and $\Delta y = 1$ mm.

great influence compared to an error on g2 position as we will see below.

4. The point heat source strength identification

In this part of the paper we describe briefly the BEM approach for point source strength identification. In the second part we give some results obtained on the experimental design presented in Section 2. Some results are presented for one or two heat sources strength estimation using the thermocouples and infrared thermographic data. The position of line sources g_1 and g_2 are now assumed to be known and we will use the exact or previously identified location.

4.1. The boundary element method for the time varying strength estimation of point heat sources

The inverse method presented here is based on BEM and is already presented and detailed in [5] for heat point source strength reconstruction. The method is based on a time regularization procedure associated to some future time steps. This association permits to stabilize the solution of the ill posed problem. In the following paragraphs we describe briefly the basis of our approach, all the details concerning BEM can be found in [12] for direct problems and in [5] for inverse problem resolution. As the aim of this paper is to present an experimental application of BEM for heat source strength identification, this part is reduced to some general concepts. All the details concerning BEM for point heat source identification are given in a previous publication [5].

4.1.1. The boundary integral equation

In terms of temperatures θ, the linear transient heat diffusion equation can be written:

$$\rho C\frac{\partial\theta}{\partial t}=\lambda\vec{\nabla}^2\theta+g \tag{2}$$

with α the thermal diffusivity, g the heat source term, θ the temperature and λ the heat conductivity.

The latter partial differential equation is linear in θ as the thermal parameters are assumed constant. Considering point M, of domain Ω of boundary Γ, integrating twice Eq. (2) weighted by a fundamental solution T^* [12], leads to the Boundary Integral Equation (BIE) for the linear transient heat conduction [12]:

$$\begin{aligned}c\theta_{M,\,t_F}&+\int_{t_0}^{t_F}\int_{\Gamma}\alpha\theta q^*\,\mathrm{d}\Gamma\,\mathrm{d}t\\&=\int_{t_0}^{t_F}\int_{\Gamma}\alpha\frac{p}{\lambda}T^*\,\mathrm{d}\Gamma\,\mathrm{d}t+\int_{t_0}^{t_F}\int_{\Omega}\alpha\frac{g}{\lambda}T^*\,\mathrm{d}\Omega\,\mathrm{d}t\\&+\int_{\Omega}\theta_0T^*\,\mathrm{d}\Omega\end{aligned} \tag{3}$$

with M a point of Γ or Ω, p the heat flux density, T^* the fundamental solution, q^* the normal derivative of T^* and c a coefficient which depends on the position of M, namely $c=1$, if M is in Ω and $c<1$, if M is on Γ (e.g. $c=0.5$ if Γ is smooth at M).

For transient and non-linear thermal diffusion (temperature-dependent conductivity), the BIE formulation is possible only if the space and time derivatives of the diffusivity are small. The fundamental solution T^* is a time-and-space-dependent Green function [13] which permits to cope with localised measurements (internal points) and singularities as heat point sources. It has to be mentioned that BEM does not require a complete domain mesh but only a boundary mesh (see [12]).

4.1.2. The heat point source treatment

If the initial temperature field is uniform or stationary, the domain integral in Eq. (3) associated to initial conditions vanishes. Nevertheless, in Eq. (3), a domain integral associated to the heat source term g still remains. Let us consider a set of K point heat sources in domain Ω; then the heat source term g in BIE (3) can be written:

$$g=\sum_{k=1}^{K}\mathbf{g}_k\delta_{M_k} \tag{4}$$

with: $\mathbf{g}_k$ the algebraic strength of the source k, δ_{M_k} the Dirac function at the location M_k of point source k.

Using the properties of point heat sources, the domain integral corresponding to the heat source in Eq. (3) can be simplified [5]. It should be noted that a line heat source in a 3D system can be represented by a point in the 2-D diffusive system; this last configuration is realized here using a thin heating wire in a long bar.

4.1.3. The discrete formulation

To discretize BIE (3), we use elements constant over space, and linear over time. This last assumption means that the temperatures and flux densities are taken to be constant on each element and linearly variable between two successive time steps. In a similar way a linear variation in time for the heat source strength $\mathbf{g}_k$ within each time step will be assumed. If the geometry, the diffusivity and the coordinates of the set of sources are known, by applying a discrete form of (3) to all N boundary nodes it is possible to calculate some time and space dependent coefficients, these coefficients are given in details in [5,12]. The calculated coefficients are gathered in matrices $\mathbf{H}$, $\mathbf{G}$ and $\mathbf{I}$. A similar formulation is used to build matrices $\mathbf{H}'$, $\mathbf{G}'$ and $\mathbf{I}'$ corresponding to the N' internal points. If we use a successive resolution procedure provided that at

time t_F all the variables are known for $t < t_F$ and if it is assumed that the N' internal temperatures are known, we can build the system:

$$\begin{bmatrix} 0 \\ T'_F \end{bmatrix} + \begin{bmatrix} \mathbf{C}+\mathbf{H} \\ \mathbf{H}' \end{bmatrix} T_F = \begin{bmatrix} \mathbf{G} \\ \mathbf{G}' \end{bmatrix} P_F - \begin{bmatrix} \mathbf{I} \\ \mathbf{I}' \end{bmatrix} S_F + \begin{bmatrix} W_F \\ W'_F \end{bmatrix} \quad (5)$$

with: T_F (T'_F) vector of dimension N of temperature on the boundary nodes at resolution time t_F, P_F: vector of dimension N of heat flux densities on the boundary nodes at time t_F, $\mathbf{H}$, $\mathbf{G}$, ($\mathbf{H}'$, $\mathbf{G}'$) matrices of dimension (N, N) ((N, N')), S_F vector of the intensity for the K point heat source at time t_F, $\mathbf{I}$ ($\mathbf{I}'$): matrix of dimension (N, K) ((N', K)), $\mathbf{C}$: diagonal matrix of dimension (N, N), W_F second member vector of dimension N containing all the information for $t < t_F$.

System (5) contains $N+N'$ equations and $2N+K$ unknowns, namely N boundary temperatures, N boundary heat flux densities and K point heat source strength.

If we can find N boundary conditions (one per element), which can be an imposed temperature, a heat flux or a combination of these two variables, the number of unknowns is reduced to $N+K$. If $N' \geq K$, (5) can be solved using a least squares method. Considering the ill-posed character of the inverse problem, as recommended in [1], we use some future time steps. Over the future time steps we use a regularization procedure similar to the sequential regularization proposed in [1].

4.1.4. Future time steps — time and space regularization procedures

The method of the future time steps consists of solving the problem at time t_F taking into account the measurements at times t_F, t_{F+1}, t_{F+2} ... t_{F+R} in order to increase the sensitivity of the solution to the measurements at time t_F. Applying this procedure we obtain a macro system including a formulation of (5) over the future time steps. If we rearrange the obtained macro-system and combine the unknowns in a vector X, we obtain:

$$\mathbf{A}X = B \quad (6)$$

with $\mathbf{A}$ a matrix of dimension (($N+N'$)(R + 1), ($N+K$)(R + 1)), X a vector of dimension (($N+K$)(R + 1)) and B a vector of dimension ($N+N'$)(R + 1). In the general case we have more measurements than unknowns ($N' > K$) and X has to minimize a cost function $J(X)$ defined as:

$$J(X) = \|\mathbf{A}X - B\|^2 \quad (7)$$

The regularization procedure, used to reduce excursions into the unknown function, is based on the regularization operator recommended by Thikonov [8] and is already applied in [5]. Let us introduce the time regularization matrix $\mathbf{Q}$ of dimension (($N+K$)(R + 1), ($N+K$)(R + 1)) and η a coefficient adjusting the amplitude of $\mathbf{Q}$. The described procedure is similar to the sequential regularization method proposed in [1] by Beck et al. For this approach described in [1], Thikonov regularization operator [8] is applied to the unknowns over the future time steps in a sequential way.

This method applied to the time dependent variables over the R future time steps is not efficient to reduce the spatial oscillations of the space dependent variables. The space regularization procedure is described in [3] for the heat flux density identification. Using a similar formulation such as described in [3,4], the space regularization matrices are gathered in a macro matrix $\mathbf{U}$ of block diagonal form associated to a coefficient μ, adjusting the amplitude of the operator. Matrices $\mathbf{Q}$ and $\mathbf{U}$ are built on the successive derivatives of the function to be regularized as recommended by Thikonov [8].

If we use a space and time regularization procedure, the system defined in Eq. (6) is modified and X has to minimize a modified cost function $J(X)$ defined as the following:

$$J(X) = \|\mathbf{A}X - B\|^2 + \mu\|\mathbf{U}X\|^2 + \eta\|\mathbf{Q}X\|^2 \quad (8)$$

If we apply the least square method (in the case of an Euclidean norm) to minimize function (8), this leads to

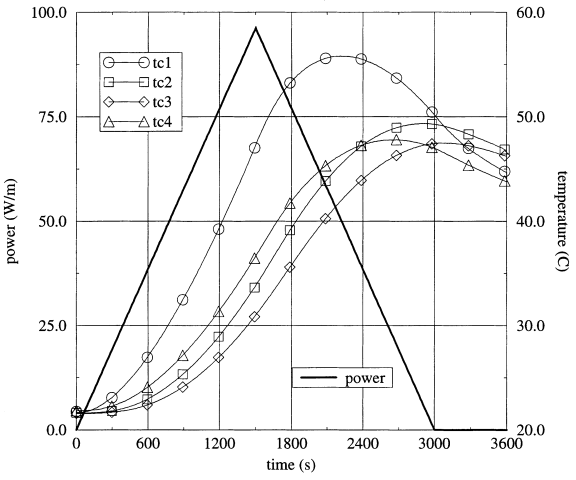

Fig. 6. Measured internal temperatures (°C) vs time (s) at the four internal sensors (375 points per curve) and experimental g2 strength (W/m) vs time.

vector X solution of the square system of linear equations:

$$(\mathbf{A}^{\mathrm{T}}\mathbf{A} + \mu\mathbf{U}^{\mathrm{T}}\mathbf{U} + \eta\mathbf{Q}^{\mathrm{T}}\mathbf{Q})X = \mathbf{A}^{\mathrm{T}}B. \quad (9)$$

A resolution of (9) is performed at each time step t_{F}. From vector X we extract component X_{F} of the unknowns at time t_{F}; the other components ($X_{\mathrm{F}+1}$, …, $X_{\mathrm{F}+\mathrm{R}}$) of X being ignored. Then the computation can be resumed for time $t_{\mathrm{F}+1}$ to work out vector $X_{\mathrm{F}+1}$ ignoring components ($X_{\mathrm{F}+2}$, …, $X_{\mathrm{F}+\mathrm{R}+1}$).

In all the following we will use a second order regularization which preserves the average of the identified function. The association of time and space permits to regularize all the unknowns: the point heat source strength in time and the identified heat flux densities over the scanned in surface space.

4.2. Experimental results of identification

In this part we present some results obtained for different identification of the strength of g_1 or g_2 or both using BEM. This paragraph is divided in four parts, the first one presents an example of measurements for a particular intensity evolution of g1 studied in the above sections. The second one concerns the identification of a single source using four sensors: it will show the importance of the source location precision. The third part presents some similar results obtained with two sensors: it will show the importance of the regularization and future time steps procedures in experimental identifications. The last section gives an example of a double source intensity identification.

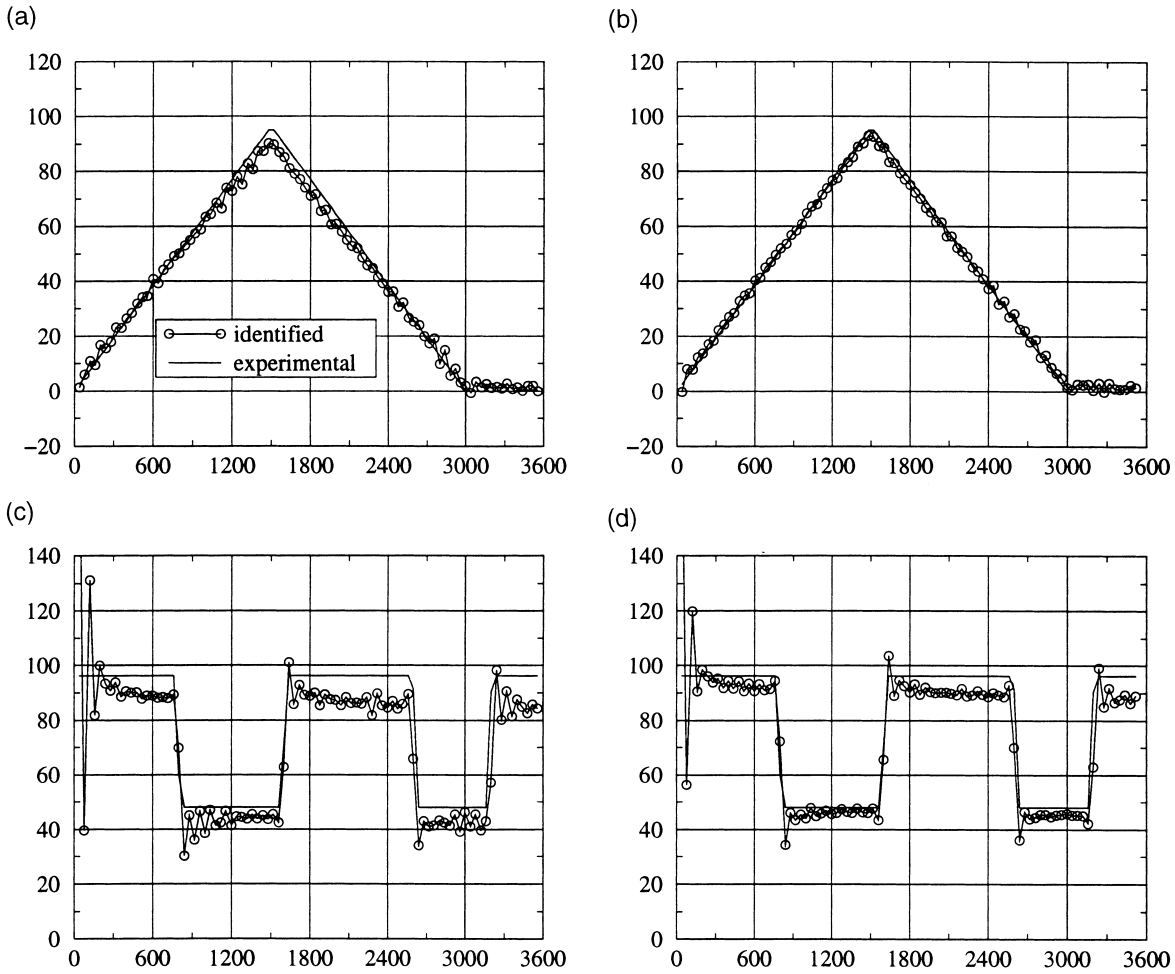

Fig. 7. Identified intensity (W m^{-1}) of g2 vs time (s) using an exact position and no regularization ($\mu = \eta = 0$). (a) Triangular, R = 3; (b) triangular, R = 6; (c) stepwise, R = 3; (d) stepwise, R = 6.

4.2.1. Example of measurements

The measurements presented in this section are used in the following sections to reconstruct the time variations of g_2. Fig. 6 presents on the same chart the temperature variations measured at sensors tc1, tc2, tc3, tc4 and the triangular power variation imposed on g_2.

As we can see at Fig. 6 sensor tc1 is very sensitive to g2 strength variations, which is explained by the short distance between the sensor and the heat source: 11.2 mm. The responses obtained at sensors tc2 to tc4 lag behind the solicitation and are damped compared to tc1. As we will see in section 4.2.3, this lack of sensitivity has a bad influence on the IHCP results. This influence will have to be balanced by the resolution parameters: the number of future time steps and the regularization parameter η.

4.2.2. Experimental intensity identification of a single source using four sensors

The example corresponding to the results displayed in Fig. 7 concerns the identification of g2 using 4 thermocouples and the exact position. Two solicitations are presented here: a triangular variation and a stepwise variation in time. It is important to notice that these results are obtained without any regularization term ($\mu=\eta=0$ in Eq. (14)). Nevertheless some future time steps are necessary to reconstruct the original signal as we can see by comparing Fig. 7(a) and (b) and also (c) and (d).

The triangular variation is better reconstruct than the stepwise variation. The total energy identified during all the time steps is 144.307 kJ m^{-1} for the triangular variation and 260.420 kJ m^{-1} for the stepwise

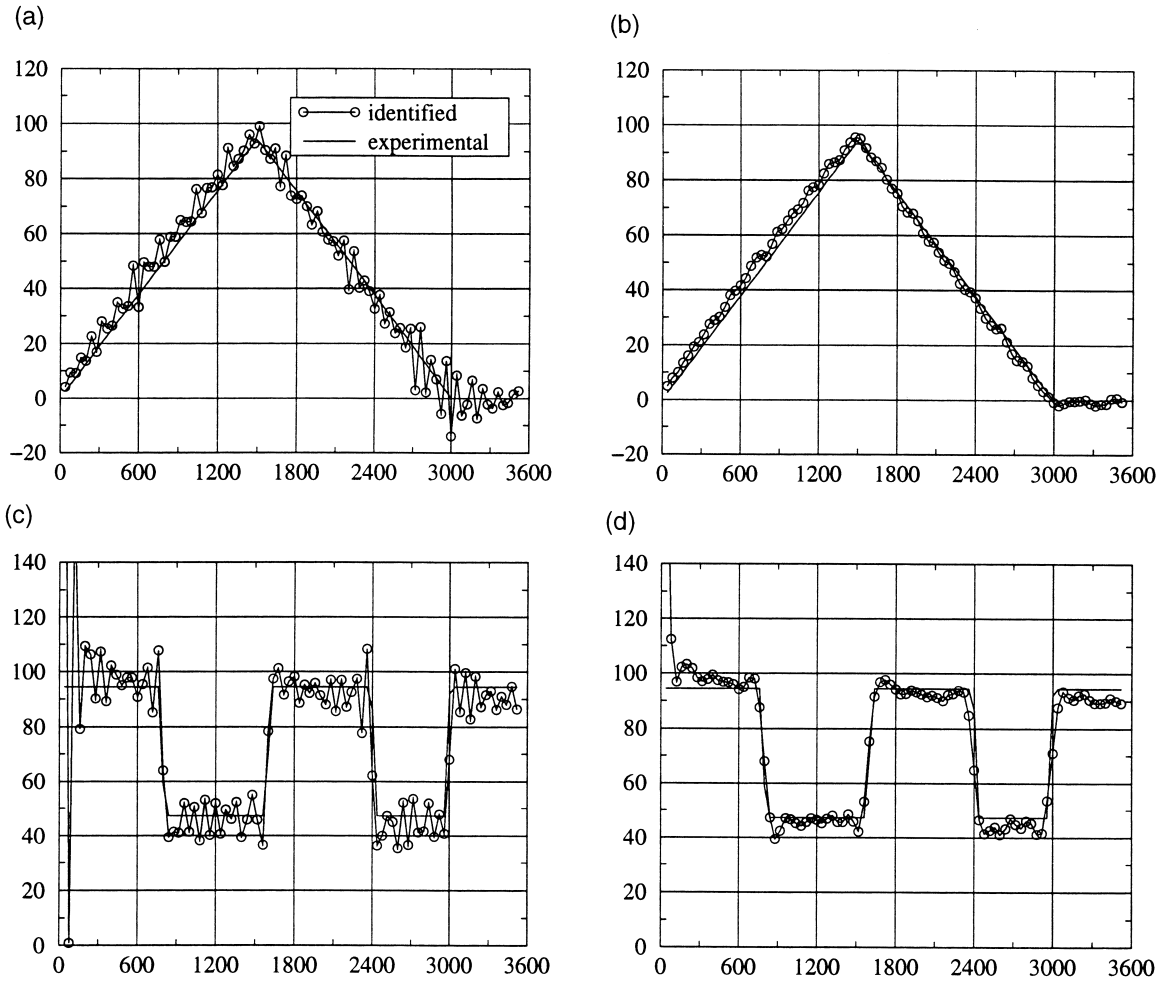

Fig. 8. Identified intensity (W m^{-1}) of g1 vs time (s) using an exact position. (a) Triangular, $R = 6$, $\eta=10^{-8}$; (b) triangular, $R = 6$, $\eta=10^{-5}$; (c) stepwise, $R = 6$, $\eta=10^{-8}$; (d) stepwise, $R = 6$, $\eta=10^{-5}$.

variation. The difference between the experimental input and the identified energy is of 0.04% in the triangular case and 4.33% in the stepwise case. This result is explained by the level of energy which is more important in the stepwise case. Thus the reconstruction is more sensitive to errors in the thermal losses through the insulation estimation and also to errors in the assumed location of the experimental source. The less good result displayed at Fig. 7(d) compared to the one displayed at Fig. 7(b) can also be explained by the shape of the function to be identified. The stepwise case is very difficult for IHCP resolution due to the damping and lagging properties of the transient diffusion equation. The presented example shows once again that inverse methods fail to well reconstruct the high frequencies flux evolution [1,2]. Nevertheless, the maximum error between estimated and measured function is less than 10%, and the total error is of 4.33% which can be considered satisfactory.

In order to compare the results obtained for g2 and g1, on the next figure we display the same results obtained in similar conditions for g1. For this example of resolution, we have chosen to present the results obtained using six future time steps and different values of the time regularization parameter η.

As we can see on Fig. 8 the results obtained for heat source identification are very sensitive to the sensor locations. Results displayed at Fig. 8 can be compared to results displayed at Fig. 7. In both Figs. 7 and 8 the stepwise variation case shows some differences between the identified part and the measured one. These differences will be explained further on by an error on the assumed exact source position.

For line source g1 (see Fig. 8) the distance from the

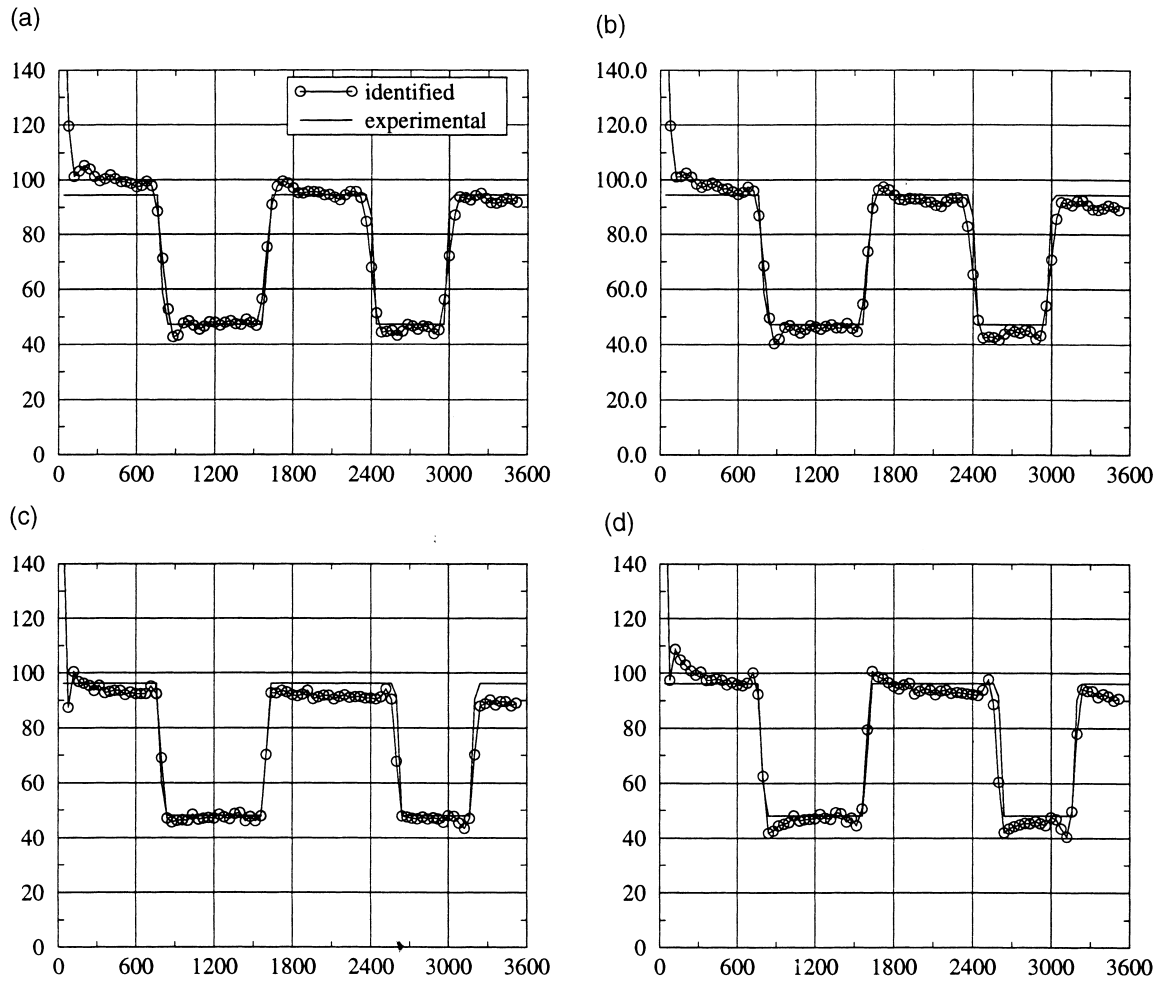

Fig. 9. Identified intensity (W m^{-1}) of unknown strength vs time (s) using an exact position with a bias of −1 mm. (a) g1, $R = 6$, $\eta = 10^{-5}$, bias on x; (b) g1, $R = 6$, $\eta = 10^{-5}$, bias on y; (c) g2, $R = 6$, $\eta = 10^{-8}$, bias on x; (d) g2, $R = 6$, $\eta = 10^{-8}$, bias on y.

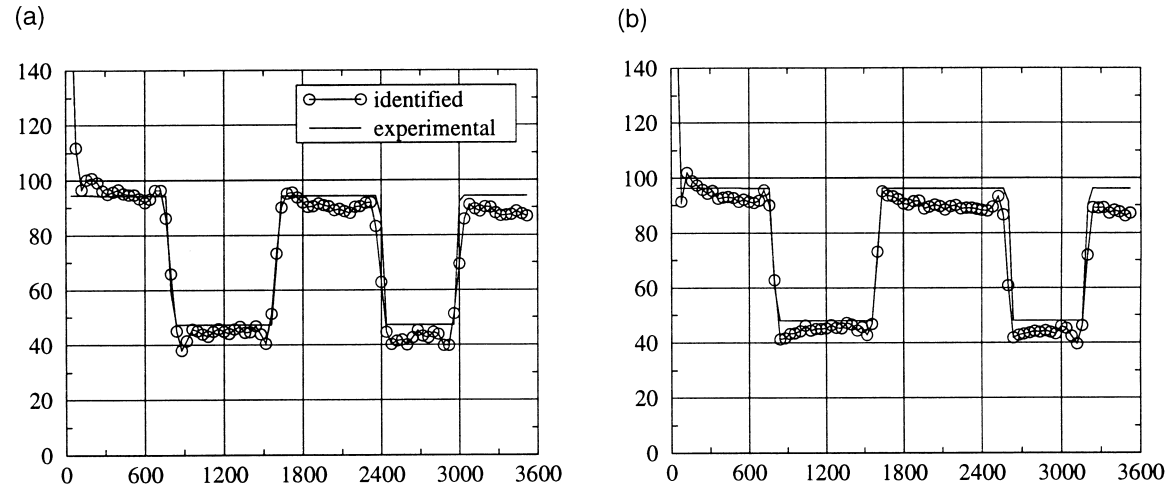

Fig. 10. Identified intensity (W m^{-1}) of g1 or g2 vs time (s) using the identified positions: g1(25.9; 24.4) and g2(15.3; 29.9). (a) g1, $R = 6$, $\eta = 10^{-5}$; (b) g2, $R = 6$, $\eta = 10^{-5}$.

sensors to the source is more important which explains the chosen number of future time steps used ($R = 6$). Here, in order to have correct results we have to use a second order time regularization, the coefficients are chosen in order to have a smooth shape. As we can see in Fig. 8(b) and (d) the increase of the regularization coefficient leads to smooth results but then the method fails to reconstruct abrupt variations of the intensity.

We have to point out that for sources g1 and g2 in the stepwise case, the first identifications are over-estimated compared to the experimental curve as we can see on Figs. 7(c) and (d), 8(c) and (d). This overestimated value is explained by the abrupt variation of power and the low level of temperature at the fist time steps. This low level leads to take into account the measurement errors as an original signal.

Before examining the case of the reconstruction using an identified position, let us consider the case of an exact position and examine the case of a 1 mm error on the position of g1 or g2 with fixed positions for the four sensors. Fig. 9 presents the results of the identification using a bias on the sources location. Considering all sensors a 1 mm error seems to be a

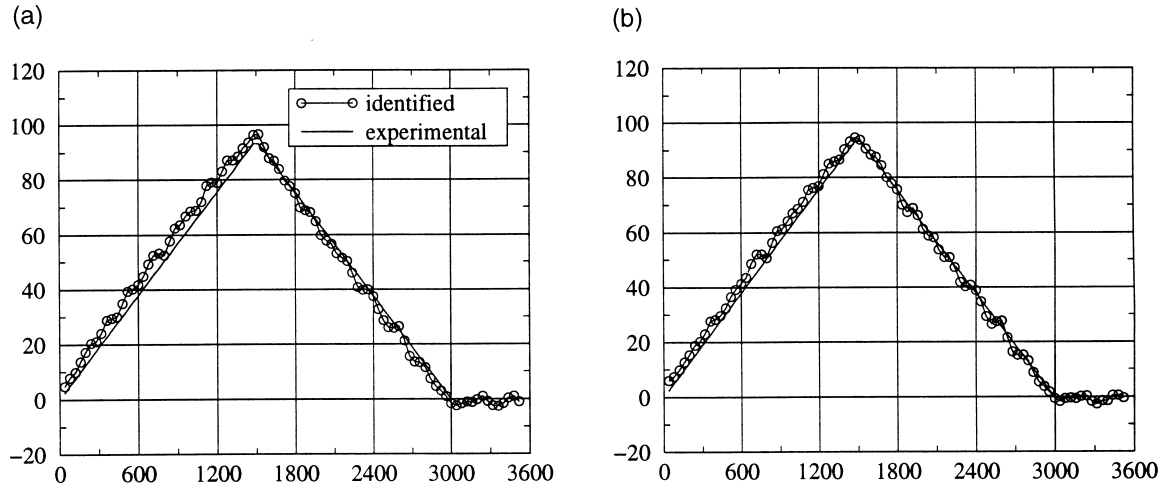

Fig. 11. Identified intensity (W m^{-1}) of g1 vs time (s) using exact position, $R = 6$, $\eta = 0$ and two sensors. (a) Sensors tc1 and tc3, $R = 6$, $\eta = 10^{-6}$; (b) sensors tc2 and tc4, $R = 6$, $\eta = 10^{-6}$.

good approximation of position error. The first column concerns an error on x of -1 mm, the second column an error on y of -1 mm, the first row concerns g1 the second one g2.

As we can see on Fig. 9 the profile of the imposed power is well recovered but the intensity profile is not perfectly reconstructed. This is especially the case for g2. Actually the sensitivity of sensor tc1 is so important that a small error on the location has a great influence on g2 strength identification. On the other hand, the g1 assumed location does not influence the reconstruction of the power because of a lower sensitivity of g1 to the measurements. If the distance between heat source and the sensor is over (under) estimated, the strength will be also over (under) estimated. This can be seen immediately by examining an analytical estimation [9] of the temperature. We have also a corrupt profile compared to the original, especially for constant profile for which the differences are easier to detect.

As shown by the sensitivity coefficients displayed at Fig. 5 the g1 strength identification is less affected by a coordinate error compared to g2 strength identification. This result is explained by coefficients contained in matrix **I**, these coefficients are a decreasing function of the distance as shown in [5]. This leads to a higher sensitivity to measurement errors but a lower sensitivity to location errors.

The last example concerns the results obtained using the best identified positions for g1 and g2, with the following coordinates:

- for g1 $x = 25.9$ mm, $y = 24.4$ mm;
- for g2 $x = 15.3$ mm, $y = 29.9$ mm

As we can see in Fig. 10(a) and (b) the original profile

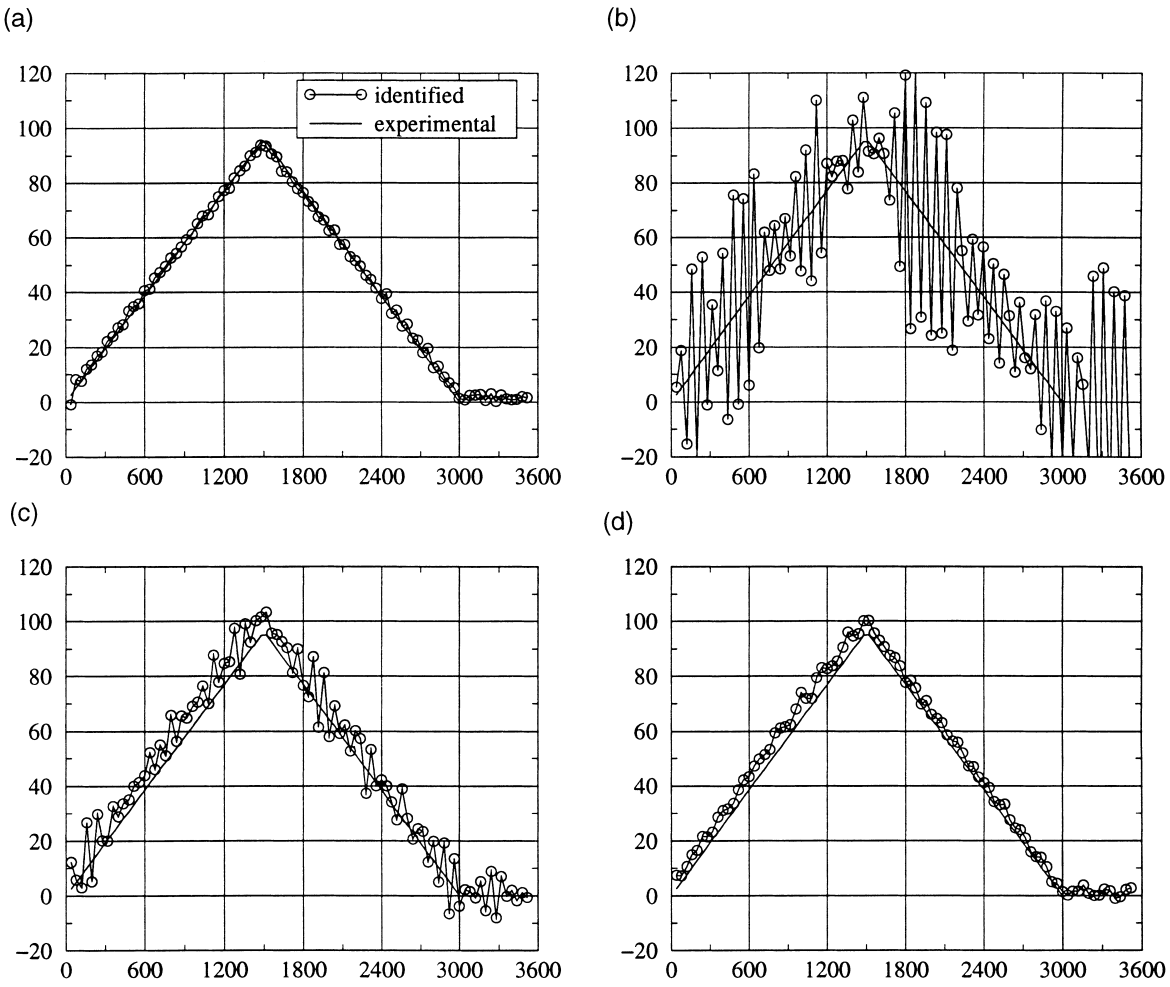

Fig. 12. Identified intensity (W m^{-1}) of g2 vs time (s) using exact position two sensors. (a) Sensors tc1 and tc3, $R = 6$, $\eta = 0$; (b) sensors tc2 and tc4, $R = 6$, $\eta = 0$; (c) sensors tc2 and tc4, $R = 6$, $\eta = 10^{-8}$; (d) sensors tc2 and tc4, $R = 6$, $\eta = 10^{-5}$.

is not well recovered which is explained by an error on location and by some inhomogeneous heat losses through the insulation.

Nevertheless, the identification results are satisfactory with for g1: a cumulative error of -176 W m^{-1} and a mean error of -2.00 W m^{-1} and for g2 a cumulative error of -425 W m^{-1} and a mean error of -4.83 W m^{-1}. At this point of the paper it is important to notice that for a single source a single sensor would be enough to solve the problem of the strength identification. In this case the location identification would not be possible. As an example, in the following paragraph we examine the case involving two sensors for the identification of a single heat source strength.

4.2.3. Experimental intensity identification of a single source using two sensors

The two pairs of sensors (tc1; tc3) and (tc2; tc4) are used. In Fig. 11 we present the results obtained for the g1 strength identification using two sensors. As the experimental set is symmetrical the results are nearly identical for the same conditions, and the differences are due to an error in the position estimation.

As we can see on Fig. 11(a) and (b) the results are very similar to those obtained with four sensors, because the indications of sensors (tc1; tc3) and (tc2; tc4) are correlated. This is not the case for heat line source g2 for which the location is not symmetrical with respect to sensors (tc1; tc3) and (tc2; tc4). In Fig. 12 we present the identification of g2 using sensors (tc1; tc3) or (tc2; tc4).

The results obtained using sensors tc1 and tc3 are good, which is not the case using sensors tc2 and tc4. If we examine Fig. 2, the indications provided by thermocouples 2 and 4 are correlated and less sensitive than indications given by thermocouples 1 and 3. In fact thermocouple tc1 would be sufficient to identify correctly g2 strength. The characteristic time value (distance$^2/\alpha$) are:

- for tc1 238 s then six time steps;
- for tc2 1382 s then 35 time steps;
- for tc3 1954 s then 49 time steps;
- for tc4 810 s then 21 time steps

In terms of number of time steps the value obtained for tc1 is very low compared to the others. In this case the time lag between the cause (g1 strength variation) and the effect (temperature measured at tc1) is short. As a result, a number of six future time steps leads to very good results without any regularization procedure. In the other cases a time regularization procedure is necessary to deal with a lack of future time steps. This is the case for results displayed in Fig. 12. It shows that using thermocouples tc2 and tc4 leads to bad results without regularization.

In system (9) the resolution performed to obtain the heat source strength displayed at Fig. 12(a) leads also to the heat flux density profile over the scanned surface. In the previous experimental studies presented in [4] the aim was the heat flux density field identification which is not the case here. Nevertheless in down to earth applications this last property can be used for the time and space identification of heat transfer coefficients by scanning the concerned surface and identifying the heat flux density field.

It can be noticed that in the case of a cylinder placed in a transient fluid flow, it is possible to identify

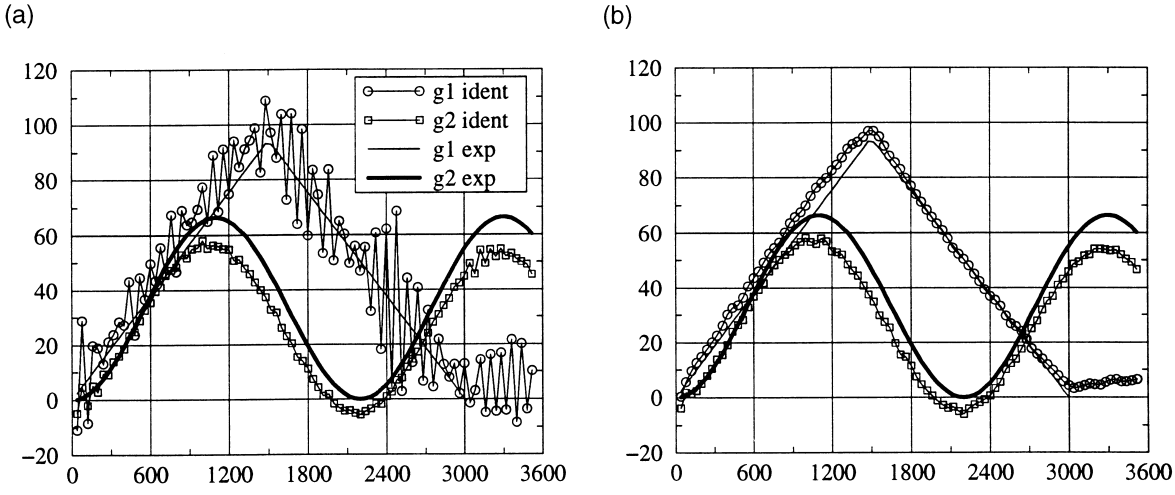

Fig. 13. Identified intensity (W m^{-1}) of g1 or g2 vs time (s) using four sensors and identified positions: g1(2.59; 2.44) and g2(1.60; 3.01). (a) $R = 6$, $\eta = 10^{-8}$; (b) $R = 6$, $\eta = 10^{-5}$.

the heat transfer coefficient at the boundary with only temperature measurements: internal temperatures in the material (in order to identify the heat line source strength) and surface temperature provided by an infrared scanner.

4.2.4. Experimental intensity identification of two sources using four sensors

For these last results we present the simultaneous identification of line heat sources g1 and g2 strength, the results using an identified location are displayed in Fig. 13. The positions used to obtain these results have been identified above (see section 3.2). The results are satisfactory but we can point out that in the reconstruction procedure, line source g1 strength is overestimated and g2 strength is underestimated. This difference is a result of the particular position of the different sensors in the bar which can lead to an almost singular resolution matrix. As the energy has to be preserved, given the temperature level and the thermal parameters, if a line heat source is over estimated, the other one will be underestimated with a global conservation along all the time steps. For the result presented below the sum of the algebraic errors on g1 is 300 W m^{-1}, the sum of the errors on g2 is -592 W m^{-1}. The global error is then of -292.26 W m^{-1} over all the time step which represent an average of -3.32 W m^{-1}. The results of the identification procedure are satisfactory but some improvements can be done in accuracy of thermocouples and line heat source locations.

5. Conclusion

In order to test our previous numerical works about heat source identifications, we set up a 2-D experiment. This one permits us first to solve a transient 2-D IHCP which consists of a point heat source location using an iterative algorithm and, when the location is known, the reconstruction of time variations of line heat source intensities. The IHCP resolution is performed using a BEM inverse formulation connecting a future time step and a regularization method. Through this experiment, we show the good potentialities of our methodology, connecting numerical and experimental approaches. In further investigations, we intend to identify multiple heat sources location and strength using infrared thermography, an application could be the non destructive control.

References

[1] J.V. Beck, B. Blackwell, C.R. St Clair, Inverse Heat Conduction, Ill-Posed Problems, Wiley Interscience, 1985.
[2] E. Hensel, Inverse Theory and Applications for Engineers, Prentice-Hall, Englewood Cliffs, 1991.
[3] R. Pasquetti, C. Le Niliot, Boundary element approach for inverse conduction problems: application to a bidimensionnal transient numerical experiment, Num. Heat Transfer, Part B 20 (1991) 169–189.
[4] C. Le Niliot, Méthode des éléments de frontière pour la résolution des problèmes inverses en diffusion thermique, University doctoral thesis, Université de Provence, Marseille, France, 1991.
[5] C. Le Niliot, The boundary element method for the time varying strength estimation of point heat sources: application to a two-dimensional diffusion system, Num. Heat Transfer, Part B 33 (1998) 301–321.
[6] C. Le Niliot, D. Petit, Y. Touhami, P. Gallet, An experimental estimation of a point heat source in a 2-D diffusion system using different numerical techniques, in: Proceedings of the Second International Conference on Inverse Problems in Engineering: Theory and Practice, Le Croisic, France, June 9–14, 1996.
[7] Y. Touhami, Identification spatio-temporelle d'une source de chaleur dans un milieu diffusif par résolution d'un problème inverse, University doctoral thesis, Université de Provence, Marseille, France, 1996.
[8] A.N. Thikhonov, V.Y. Arsenin, Solutions of Ill-Posed Problems, VH Winston & Sons, Washington, DC, 1977.
[9] H.S. Carslaw, J.C. Jaeger, Conduction of Heat in Solids, Oxford University Press, 1959.
[10] J.V. Beck, K.J. Arnold, Parameter Estimation in Engineering and Science, John Wiley & Sons, New York, 1977.
[11] R. Taktak, J.V. Beck, E.P. Scott, Optimal experimental design for estimating thermal propeties of composite materials, Int. J. Heat Mass Transfer 36 (12) (1993) 2977–2986.
[12] C.A. Brebbia, J.C.F. Telles, L.C. Wrobel, Boundary Element Techniques, Springer-Verlag, 1984.
[13] M.N. Ozisik, Heat Conduction, 2nd ed., John Wiley & Sons, New York, 1993.